Physical Water Treatment using Alternating Variable Frequency Electric Field Device for the Mitigation of Limescale in Industrial Production.

Ye Zhang
Northeast Electric Power University
Shengxian Cao (csxlb_jl@163.com)
Northeast Electric Power University
Yunhan Wang
Northeast Electric Power University
Gong Wang
Northeast Electric Power University
Tianyi Sun
Northeast Electric Power University

Research Article

Keywords: Alternating variable frequency electric field, Industrial scale inhibition, Field test, Energy saving

Posted Date: January 27th, 2021

DOI: https://doi.org/10.21203/rs.3.rs-152172/v1

Physical water treatment using alternating variable frequency electric field device for the mitigation of limescale in industrial production.

Authors:

1) Ye Zhang E-mail: zhangyecy@163.com

2) Shengxian Cao* E-mail: csxlb_jl@163.com

3) Yunhan Wang E-mail: wangyunhan0611@163.com

4) Gong Wang E-mail: wg_neiep@163.com

5) Tianyi Sun E-mail: ssttyy313@163.com

All Authors affiliation: Northeast Electric Power University

Postal address of the corresponding author: Northeast Electric Power University, 169 Changchun Road, Chuanying District, Jilin City, Jilin Province, China

Abstract:

Electric field scale inhibition is one of the most promising methods of scale inhibition. In this study, an alternating variable frequency electric field device is presented, it able to prevent the growth of scale in industrial heat exchange equipment effectively. Conduct field test at the heat exchange station to analyze the scale inhibition performance of the device. The test results showed that after using alternating variable frequency electric field device, the scale thickness on the heat exchange surface is significantly reduced, fouling resistance reduced by more than 58%, and the anti-corrosion rate for Fe element content reaches 19.78%, The SEM image of the scale changes from a dense irregular sharp shape to a loose spherical shape. Conclusively, alternating variable frequency electric field device has grate scale inhibition performance. This is of great significance to the field of heat transfer and energy saving.

Keywords: Alternating variable frequency electric field; Industrial scale inhibition; Field test; Energy saving.

1 Introduction

Scale refers to the crusty chalky or soft muddy substances that gradually accumulates on the solid surface in contact with mineral ion-containing fluids[1]. Industrial and domestic water contains excessive mineral ions. Scale species differs from depending on the treatment method and mineral content of the utilized water. Among them, the most common mineral ions are Ca^{2+} and Mg^{2+}[2]. When the hard water

flows through the heat transfer equipment, these ions and bicarbonate ions precipitate due to changes in pressure and solubility,, eventually forming mineral deposits(limescale) on the heat transfer surface. a process traditionally called “fouling” (Reaction (1)) [3-4].

$$Ca^{2+} + 2HCO_3^- \rightleftarrows CaCO_3(s) + H_2O + CO_2(g) \quad (1)$$

Fouling phenomena are widespread in the heat transfer process of industrial production[5-6]. Examples include thermal power, petroleum, desalination, and food industries. Scale forms on a heat exchange surface is harmful. Firstly, Once scale forms in the pipe, the water flow area gradually decreases until it is completely blocked[7]. Secondly, since the thermal conductivity of scale deposits are much lower than that of metals, scaling not only seriously affects the heat transfer efficiency of the heat exchanger[8-9] but also lead to system operation malfunction easily[10]. Lastly, the adhesion of scale causes the metal on the heat transfer surface to corrode[11], thereby triggering safety accidents such as pipeline perforation. Thus, it is self-evident that if one can reduce scale on heat transfer surface during production process, the saving in energy, safe and high-speed production, and maintenance of equipment will be truly significant.

At present, the common scale inhibition technology in the industry are the use of chemical reagents[12], such as ion exchange method that using ion exchange resin to replace scaled cations (calcium ions, magnesium ions, etc.) from hard water. Or add scale inhibitor[13-14] to the hard water to inhibit the growth of scale. Even though all the above chemical scale-removing methods are effective, long-term use causes chemicals to residue in the water, affecting the environment and even human health. Furthermore,

once scale on the heat transfer surface, that requires several methods to removal scale such as chemical cleaning[15], mechanical cleaning[16], and high-pressure jet cleaning, etc. This not only leads to economic losses caused by shutdowns, but also mechanical strength affects the service life of pipe and equipment. Therefore, an energy-saving, efficient, environmentally-friendly, and scale inhibition technology that does not affect normal production is a new research direction.

The physical method of scale inhibition is a green and pollution-free water treatment method[17], such as solenoid coils[18-19], catalytic materials[20], magnetic fields[21], electric fields[10], ultrasonic waves and electromagnetic fields[22]. Among them, the electric field scale inhibition method is a new research hotspot, and the scale inhibition effect is more obvious. Leonard D et al. [5]used RF electric field for physical water treatment to reduce calcium carbonate scale in the cooling water, they introduced the RF electric field into the cooling water through a set of parallel graphite electrode plates, the experimental results showed that the high frequency signal with frequency of 13.56MHz and 27.12MHz has better scale inhibition effect at 2V, 5V and 13V. Wontae Kim et al. [23] inserted dual electrodes into the pipe to inhibit mineral scale and bio-scale in the heat exchanger, and the results showed that this method can maintain the heat transfer coefficient of the heat exchanger at 90% (close to no scale).

At present, almost all such researches are configuration with artificial hard water in the laboratory, and the scale component is single, such as a single $CaCO_3$, $MgCO_3$, etc., and does not involve testing and application in industrial production. In real industrial production, circulating water has more complex chemical composition and

the scale composition rather than a single mineral deposit. The environmental factors that affect the growth of scale are also particularly complex, such as temperature, pressure, and flow rate. Thus, the development of a device that can effectively inhibit scale in a complex industrial environment is the focus of current electric field scale inhibition research. After almost 10 years of continual research and field experimentation, an electric field inhibition scale device has been developed which, not only collects the advantages of traditional electric field scaling technology, but also make up for their shortcomings. Therefore, the objective of this paper is to introduce the working principle of the device and to conduct experiments on scale inhibition effect in industrial production.

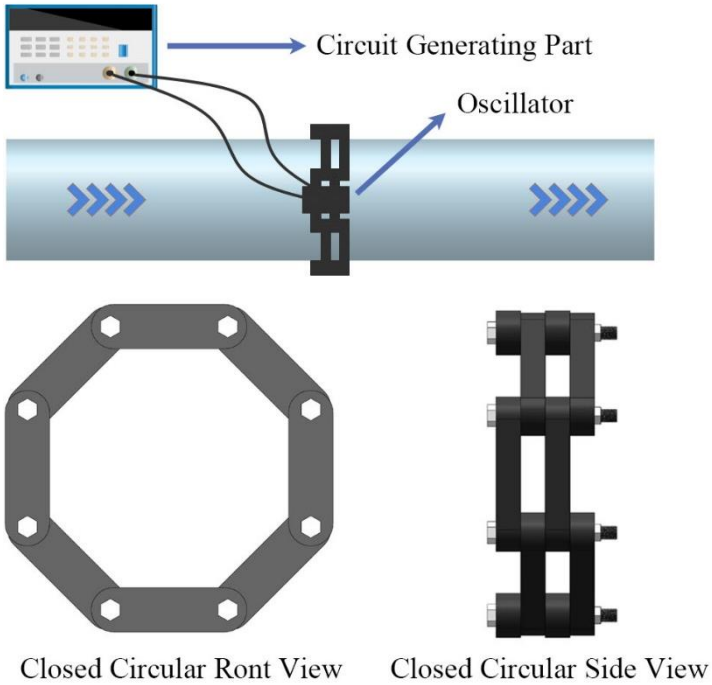

Fig.1. A diagram of the alternating variable frequency electric field device schematic

2 Materials

2.1 Device composition and working principle

A diagram of the alternating variable frequency electric field device schematic is presented in Fig. 1. The device consists of an electric field source and a coupled transducer, among them the coupled transducer includes an oscillator and a closed magnetic ring. The electric field source and the coupled transducer are designed to be separated and connected by wires to facilitate field installation. When installed, the oscillator is nested in the closed magnetic ring, which surrounds the outer wall of the pipe. The magnetic strips of the closed magnetic ring are connected by nylon screws, and the number of rings is determined by the outer diameter of the pipe. For example, the outer diameter of the pipe in this paper is 200mm, and the double-layer 8-ring spliced closed magnetic ring is selected.

The minerals in the water are in the form of ions, thus as Ca^{2+}、Mg^{2+}、Cl^{-}、CO_3^{2-} etc. Fig.2 is a schematic diagram of ion movement in water no applying electric field and applying electric field, in the absence of external disturbance conditions such as an electric field, ions will accumulate on the pipe wall to nucleate and crystallize, and the scaled ions in the water will adhere and deposit on the crystal surface to form scale. However, after these ions are subjected to the electric field before nucleation, the ions quickly change the direction of motion causes the positive and negative ions to collide, nucleate, adhere , crystallize in the water, and are removed by the shear force of the water without scaling on the inner surface of the tube wall.

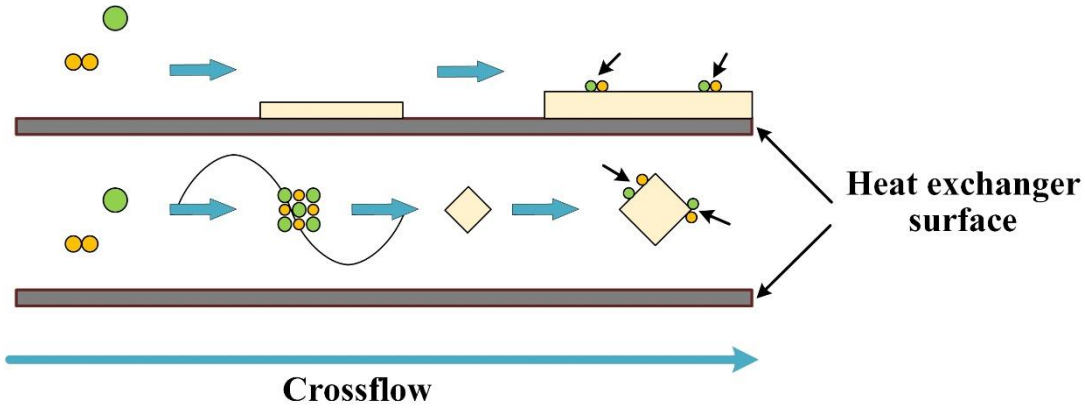

Fig.2. Schematic diagram of electric field inhibition scale process

2.2 Design of electric field source

The alternating variable frequency electric field source is generated by an electronic circuit with the function of adjusting current and frequency, which requires the excitation source to simultaneously generate both frequency modulation (FM) and amplitude modulation (AM) current signals. When this current signal passes through the coil of the oscillator in the coupled transducer, a time-varying electric field is generated in the coil. When the electric field is applied to the closed magnetic ring through the oscillator, a time-varying magnetic field is generated in the magnetic ring. According to Biot-Savart's law and Maxwell's theory, the electric field is finally applied to the fluid in the pipe through the magnetic ring.

In this process, the role of the coupled transducer is to complete the conversion of electric field-magnetic field-electric field, avoiding direct application of electric field to the water to damage the circulatory system equipment.

After years of trial and error and comparison of effects, a damped cosine wave whose peak-to-peak value gradually decreases from 70V to 5V is used as a periodic non-uniform electric field signal. In order to prevent the device from affecting the scale

inhibition effect due to the memory of the water after long-term to use, the frequency selection varies randomly within the range of 80kHz-300kHz with grate scale inhibition effect. This process is realized by the circuit applying formula (2) underdamped attenuated oscillation signal to the coupled transducer. ω and φ randomly change according to the law within a specific range. The waveform of this signal is shown in Fig.3, when the wave reaches the output terminal, a negative sharp pulse appears, there is a long tail phenomenon.

$$x = A\exp(-\delta t)\cos \omega t + \varphi \quad (2)$$

Where A represents the basic starting phase; δ is the damping coefficient; ω is the angular frequency; φ is the phase. Use the oscilloscope model of Lecory354a to test the real waveform output as shown in Figure 4.

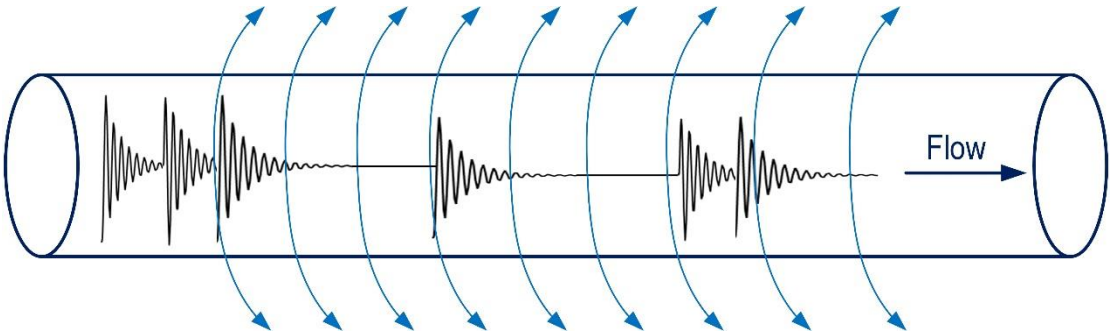

Fig.3. A diagram of the waveform of underdamped attenuated oscillation signal

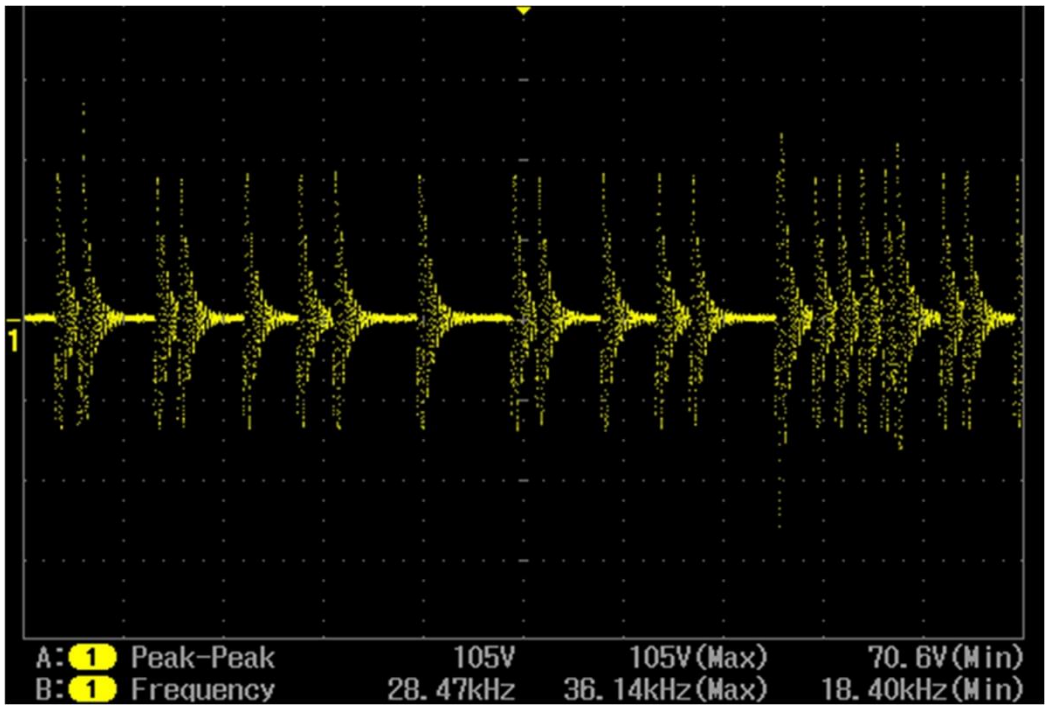

Fig.4. A diagram of the underdamped attenuated oscillating signal waveform in oscilloscope

2.3 Design of coupled transducer

The coupled transducer is an important part of introducing electric field energy into the circulating water system, it consists of an oscillator and a closed magnetic ring. The design of the coupled transducer has an important influence on the treatment effect of the device.

According to Maxwell's equation, when the alternating current generated by the electric field source powers the oscillator, the electric field and magnetic field will establish the following relationship (3) inside the coil:

$$\oint_c \vec{E} \cdot \mathrm{d}\vec{l} = \mathrm{i}\omega \mathrm{Bs} \tag{3}$$

Relating the electric field strength and magnetic field strength to the applied current, the above formula (4) can be expressed as:

$$\mathrm{E} = \mathrm{i}\omega \mathrm{B}\frac{r}{2} \tag{4}$$

Where E represents the induced electric field vector; B is the magnetic field strength vector; ω is the angular velocity of alternating current; s is line vector along the circumference ; i is an imaginary number; r is the distance from the center line of the coil to this point.

Remove the imaginary part from the equation and replace B with Iμ_0 n to get the following equation (5):

$$E = \omega I \mu_0 n \frac{r}{2} \tag{5}$$

The electric field vector in equation (12) can be regarded as a concentric circle with a radius r (distance from the center line of the solenoid).

Changing the frequency and current amplitude will change ω and I respectively, at this time, the electric field strength and magnetic field strength at any point inside the coil also change accordingly. However, it should be noted that the B and E vectors are always zero on the center line and reach their maximum values at the outer edge of the coil. When the closed magnetic loop penetrates the coil, the closed magnetic loop generates a magnetic field with the same law as the electric field in the coil.

Industrial circulating cooling water generally contains various inorganic salts. Therefore, it can be regarded as a conductor. Nesting the closed magnetic ring on the pipe of industrial water can generate induced electromotive force in the fluid, and then generate electric field. The energy transmission efficiency of the coupled transducer is closely related to the performance of the magnetic strip material that forms the closed magnetic ring. Mn-Zn ferrite R100K material and Mn-Zn ferrite MXO-400 material are two commonly used magnetic materials. The Ansys Maxwell software was used to

simulate the magnetic field intensity distribution of the two materials. Since the purpose of the simulation is to analyze the performance of two magnetic materials, it is not directly related to the number of closed magnetic loops, in order to simplify the simulation steps, the model is set to 4 loops. The simulation results in Fig. 5.

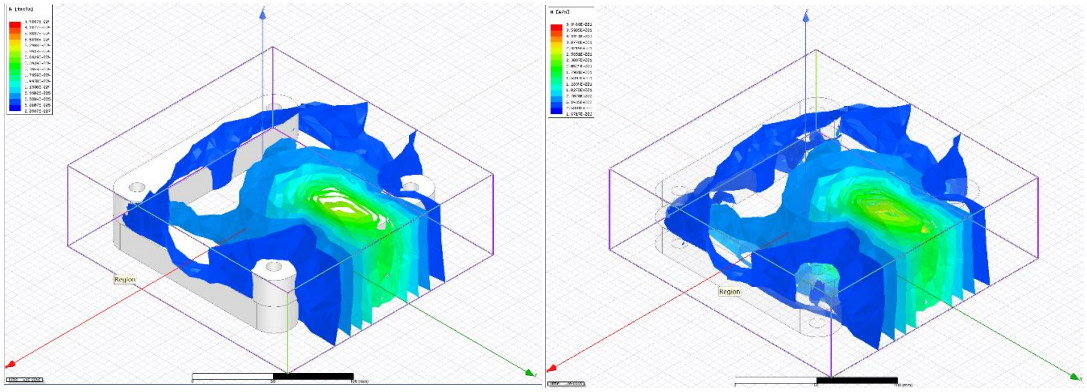

(a) material of MXO-400 (b) material of R100K

Fig.5. Magnetic field intensity distribution of two ferrite materials

From Fig.5, the clearly shows that the ferrite R100K material produces a higher and dense magnetic field strength at the selected frequency, while the MXO-440 magnetic field strength is lower and sparse. The analysis shows that R100K has a better transduction effect on the selected frequency.

3 Methods

3.1 Test procedure

In order to test the scale inhibition performance of the device in industrial production, field test was carried out. Field test at Sunshine Heat Exchange Station in Shuangliao City, Jilin Province. A diagram of the scale inhibition test flowloop is presented in Fig.6. The flowloop consists of a water circulation loop, an alternating variable frequency electric field device, a RTD temperature sensor, heat exchanger A and B, pressure sensor, water supply tank, water pump and Programmable Controllers(PLC) monitoring system. Among them, the device is installed on the

primary network water supply pipeline of heat exchanger B, and the device is not installed on heat exchanger A. A diagram of the field test installation is presented in Fig.7. 7A is the installation diagram of the alternating variable frequency electric field device, and 7B is the working voltage, current and power of the device.

The circulating water used in the test is municipal tap water. Two sets of plate heat exchangers A and B of the same batch and model are selected in the test. Table 1 lists the parameters of plate heat exchanger. Before the test, the two heat exchangers were thoroughly cleaned. After 750 hours, the test system runs stably, at this time, install the device at the water inlet of the primary network of heat exchanger B. The system records the primary network supply and return water temperature, the secondary network supply and return water temperature, t the primary network supply and return water pressure, the secondary network supply and return water pressure through the programmable controller (PLC) monitoring system of the heat exchange station. Table 2 lists the parameters of experimental system operating.

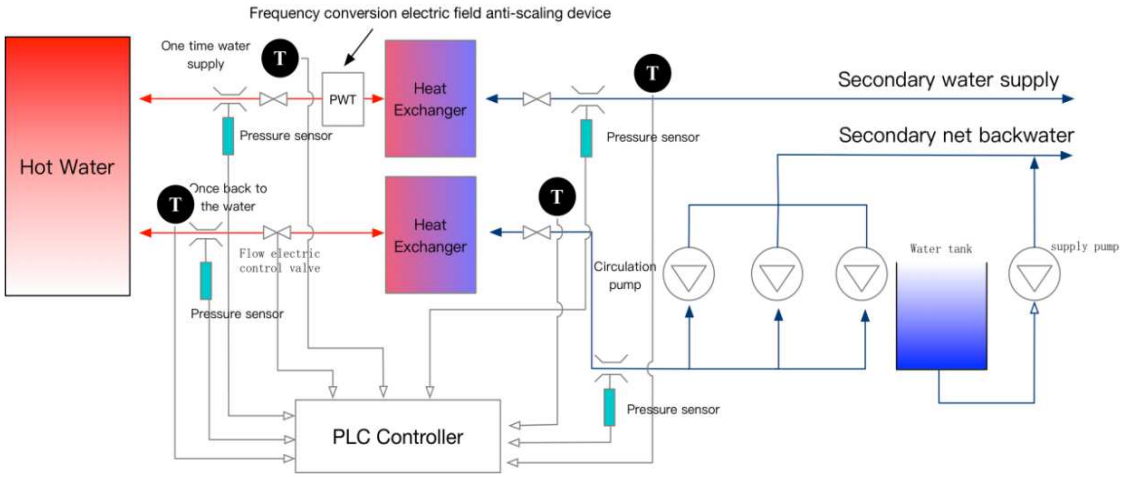

Fig.6. A diagram of the scale inhibition test flowloop

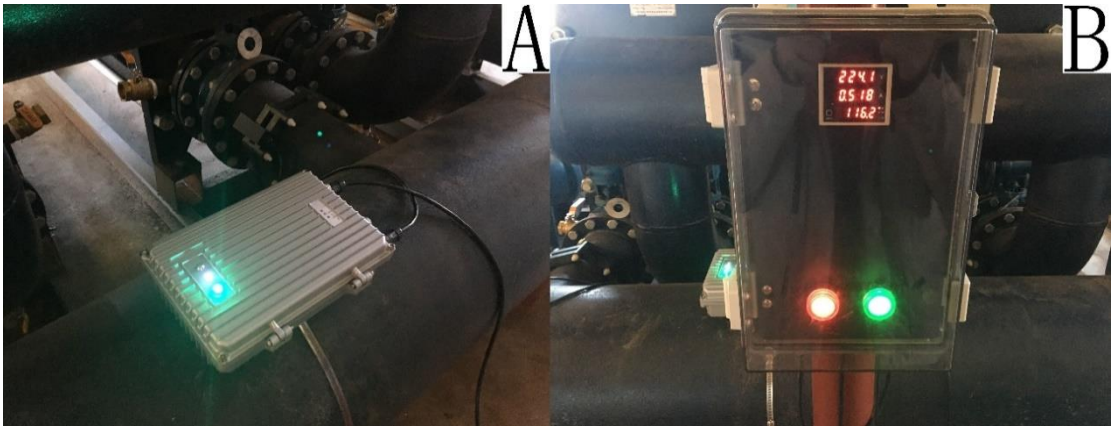

Fig.7. A diagram of the field test installation

4 Results and discussion

4.1 Analysis of scale thickness on heat transfer surface

After the test was carried out stably for 1600 hours, shut down and check the scale thickness on the surface of the two heat exchanger.

After measurement, the scale thickness of heat exchanger A is about 2~3mm, and Fig. 8A observes that the scale was hard, tightly attached to the surface of the plate heat exchanger and the heat exchanger surface has been corroded; the scale thickness of heat exchanger B is about 0.8mm, Fig. 8B clearly observes that the scale loosely floats on the surface of the heat exchanger and tends to fall off, and the metal su.rface of the heat exchanger is bright and flat. Calculated by formula (6), the scale inhibition rate is about 68%.

$$\mathrm{v}_T = \frac{T_1 - T_2}{T_1} \times 100\% \tag{6}$$

Where v_T represents the scale inhibition rate; T_1, T_2 is the scale thickness of heat exchanger A and scale thickness of heat exchanger B, respectively.

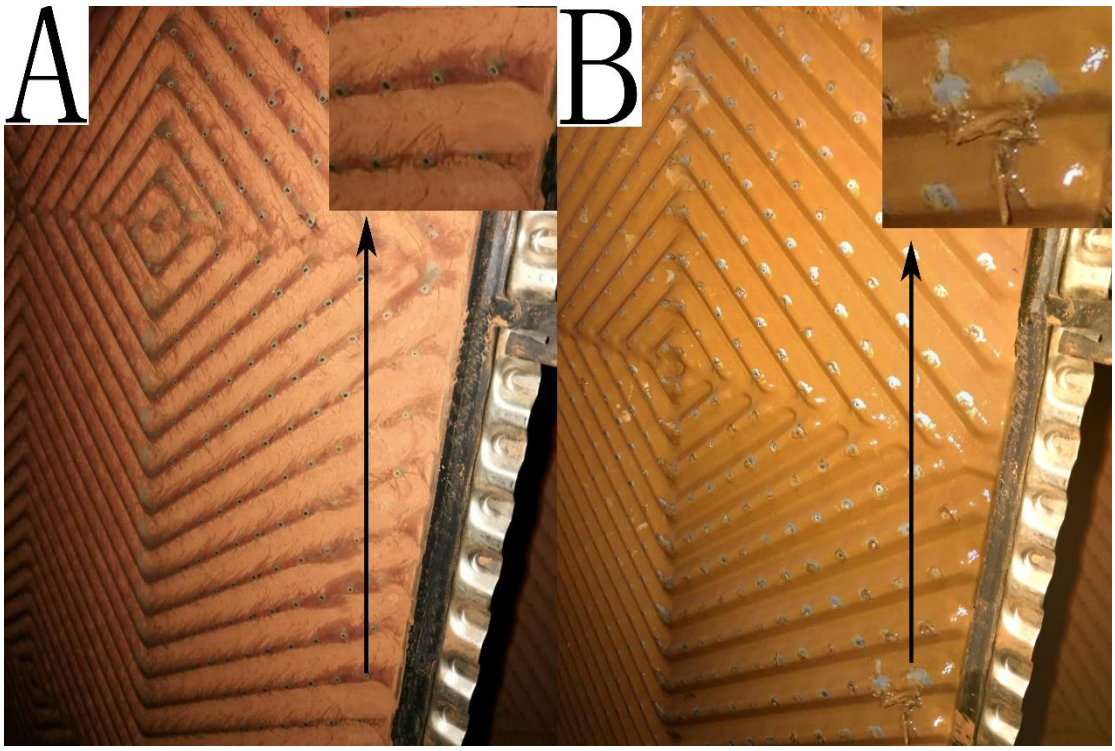

Fig.8 Comparison of scale of plate heat exchangers

4.2 Analysis of fouling resistance on heat exchange surface

Fouling resistance R_f（m^2KW^{-1}）on the surface of the plate heat exchanger, which can be defined as formula (7)[24-25]:

$$R_f = \frac{1}{U_f} - \frac{1}{U_I} \tag{7}$$

Where U_f represents the total heat transfer coefficient of scale;U_I is the total heat transfer coefficient of clean surface.

The total heat transfer coefficien U_f can be expressed as formula (8):

$$U_f = \frac{Q}{A(\Delta T_{LMTD})} \tag{8}$$

Where Q represents the heat transfer between the fluid and the heat exchange surface; A is the total heat transfer area; ΔT_{LMTD} is the log mean temperature difference;

In the test, the primary network and the secondary network are parallel flow. ΔT_{LMTD} can be expressed as formula (9):

$$\Delta T_{LMTD} = \frac{(\Delta T_{hi}) - (\Delta T_{ho})}{\ln\left[\frac{\Delta T_{hi}}{\Delta T_{ho}}\right]} \tag{9}$$

Where ΔT_{hi} represents the temperature difference between cold and hot fluid inlet; ΔT_{ho} is the temperature difference between cold and hot fluid outlet;

As an observation point every 100 hours, calculate the average fouling resistance. The fouling resistance of heat exchanger A and B is shown in Fig. 9 and Table 3. From Fig.9, as the experiment progresses, the fouling resistance of heat exchanger A continues to increase steadily, the fouling resistance of heat exchanger B only increases in the initial stage of installation of the device, and the fouling resistance remains stable with the continuous action of the electric field. Calculate the reduction rate of fouling resistance by formula (10): the fouling resistance of heat exchanger B decreased by 21% compared with heat exchanger A in the first 100 hours; after the system stabilized, it dropped by about 58%.

$$v_R = \frac{R_1 - R_2}{R_1} \times 100\% \tag{10}$$

Where v_R represents the reduction rate of the fouling resistance; R_1 is the fouling resistance of heat exchanger A; R_2 is the fouling resistance of heat exchanger B.

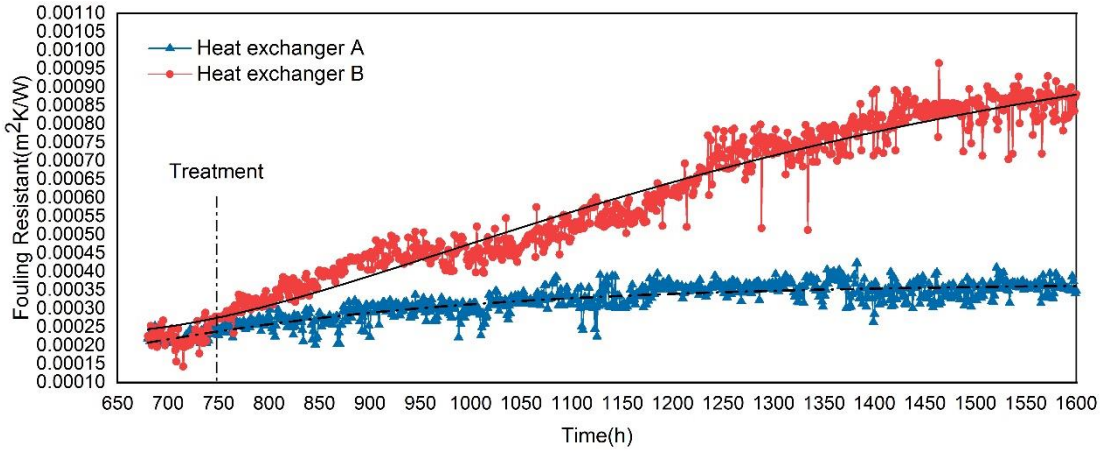

Fig.9 Changes in the fouling resistance on the heat exchanger surface in the test

4.3 Scanning electron microscope (SEM) and X-ray energy spectroscopy (EDS) analysis of scale on the heat transfer surface.

The SEM image of scale on the surface of heat exchanger shows in Fig.10. In Fig.10A, the morphology of the scale sample of heat exchanger A is mainly irregular and sharp, dense clusters, and sharp edges. In Fig.10B, the scale sample morphology of heat exchanger B is mainly spherical, with loose clusters and small particles. The scale crystals of heat exchanger A conform to the characteristics of calcite, which the growth rate of the long axis of the crystal is faster than the short axis. it is easy to produce adhesion between crystals, which gradually aggravates the scaling phenomenon. The scale crystals of heat exchanger B belong to the orthorhombic system, its growth rate in each axis is the same and forms spherical crystals and conform to the characteristics of aragonite, which the adhesion between the crystals is weakened and it is easy to leave the heat exchanger surface with the fluid flow.

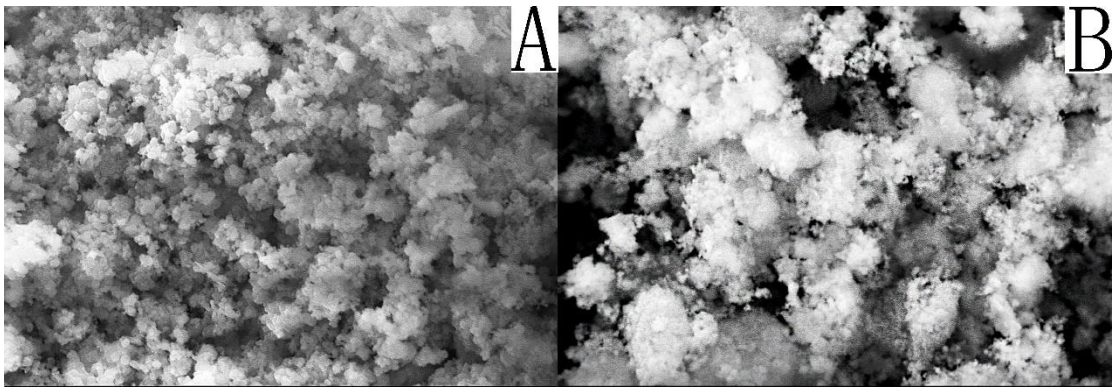

Fig.10 SEM image of scale on heat exchanger surface

A diagram of the EDS on the surface of heat exchanger A and B is presented in Fig.11, the EDS data analysis and variation of scale are shown in Table 4. In Fig,11A, the scale of heat exchanger A contains more Fe element, combining with the scale on

the surface of heat exchanger A, it is inferred that the possible cause is that the scale is completely dense during growth and the resulting alkali corrosion. The circulating water is alkaline, which causes the heat exchange wall metal, scale and circulating water to form a chemical battery, causing oxygen-consuming corrosion (the scale is the anode and the metal is the cathode).

In Fig,11B, there is relatively little Fe in the scale of heat exchanger B, combined with the scale on the surface of heat exchanger B, it is inferred that there is no metal corrosion on the surface of heat exchanger B. Besides, the EDS image shows that the C and O in the scale increase more, but the Ca and Si elements hardly increase. A possible inference is that due to the large reduction of Fe in heat exchanger B, the mass proportion of other elements in the scale increases, such as the sum of the increase in the mass fraction of C, O, Si, Ca and Cu is equal to the decrease in the mass fraction of Fe. Combined with scaling phenomenon and the SEM analysis, the alternating variable frequency electric field device only changed the form of scale molecules and reduced the corrosion phenomenon associated with scale, but did not change the chemical composition of circulating water.

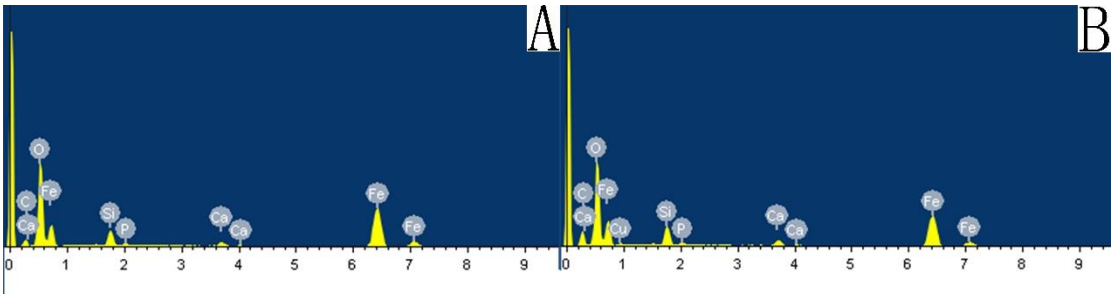

Fig.11 Comparison of EDS of scale on heat exchanger surface

5 Conclusions

In this paper, we have developed an electric field scale inhibition device that can

be used in industry. Perform performance tests on the site of the running heat exchange station, The results show:

(1) By analyzing the change of the scale thickness and the fouling resistance of the heat exchange surface, SEM and EDS analysis, it is concluded that the alternating variable frequency electric field device scale inhibition performance very well;

(2) The analysis of heat exchanger scale thickness and fouling resistance change shows that the scale inhibition rate of this device is 58% and 68% respectively;

(3) The SEM analysis shows that the scale treated by the device has a spherical shape and an orthorhombic crystal structure. Besides, the adhesion between the crystals is weakened, and it is easy to leave the surface of the heat exchanger with the flow of water, so as to achieve the effect of scale inhibition and corrosion protection;

(4) The EDS analysis shows that this device scale inhibition effect is well, reduces electrochemical corrosion phenomenon, and the antiseptic rate for Fe element content reaches 19.78%.

Acknowledgements

This work was supported by the technology research projects of department of science and technology of Jilin Province (Grant number 20190303023SF) ,and science and technology innovation development plan projects of Jilin city (Grant number 20175023).

References

[1] D. Georgiou, D. Bendos, M. Kalis, C. Koutis(Eds.), Removal and/or prevention of limescale in plumbing tubes by a radio-frequency alternating electric field inductance device. Journal of Water Process Engineering 22 (2018) 34–40. https://doi.org/10.1016/j.jwpe.2017.12.013

[2] K.H. Teng, S.N. Kazi, A. Amiri, A.F. Habali(Eds.), Calcium carbonate fouling on double-pipe heat exchanger with differentheat exchanging surfaces. Powder Technology 315 (2017) 216–226. https://doi.org/10.1016/j.powtec.2017.03.057

[3] Y. Sano, D.Nakashima. Prevention of calcium carbonate scale using electrolyzed water. International Journal of Heat and Mass Transfer 127 (2018) 1147–1156. https://doi.org/10.1016/j.ijheatmasstransfer.2018.08.070

[4] T.M. Pääkkönen, M. Riihimäki, C.J. Simonson, E. Muurinen(Eds.), Crystallization fouling of CaCO3– Analysis of experimental thermal resistanceand its uncertainty. International Journal of Heat and Mass Transfer 55 (2012) 6927–6937. https://doi.org/10.1016/j.ijheatmasstransfer.2012.07.006

[5] L.D. Tijing, H.Y.Kim, D.H.Lee. Physical water treatment using RF electric fields for the mitigation of CaCO3fouling in cooling water. International Journal of Heat and Mass Transfer 53 (2010) 1426–1437. https://doi.org/10.1016/j.ijheatmasstransfer.2009.12.009

[6] A. Janzen, E.Y. Kenig. Analysis of crystallization fouling in electric water heating. Heliyon 5 (2019) e02695. https://doi.org/10.1016/j.heliyon.2019.e02695

[7] M.N. Frota, E.M. Ticona, A.V. Neves, R.P. Marques(Eds.), On-line cleaning technique for mitigation of biofouling in heatexchangers: A case study of a hydroelectric power plant in Brazil. Experimental Thermal and Fluid Science 53 (2014) 197–206. https://doi.org/10.1016/j.expthermflusci.2013.12.006

[8] T.R. Bott, Fouling of Heat Exchangers, Elsevier Science B.V., The Netherlands, 1995. https://doi.org/10.1016/B978-0-444-82186-7.X5000-3

[9] Y.I. Cho, B.G. Choi, Electronic anti-fouling technology to mitigate precipitationfouling in plate-and-frame heat exchangers, Int. J. Heat Mass Transfer 41 (17)(1998) 2565–2571. https://doi.org/10.1016/S0017-9310(97)00347-5

[10] L.D. Tijing, D.H. Lee, D.W. Kim, Y.I. Cho (Eds.), Effect of high-frequency electric fields on calcium carbonate scaling. Desalination 279 (2011) 47–53. https://doi.org/10.1016/j.desal.2011.05.072

[11] M. F. Humphrey, Cooling Tower Water Conditioning Study. Ozone: Science & Engineering.3(2) (1981)109-119. https://doi.org/10.1080/01919518108550913

[12] S.S. Al-Jaroudia, A. Ul-Hamid, J.A. Al-Matar, Prevention of failure in a distillation unit exhibiting extensive scale formation. Desalination 260 (2010) 119–128. https://doi.org/10.1016/j.desal.2010.04.055

[13] K.H. Teng, A.Amiric, S.N. Kazi, M.A. Bakar(Eds.), Retardation of heat exchanger surfaces mineral fouling by water-baseddiethylenetriamine pentaacetate-treated CNT nanofluids. Applied Thermal Engineering 110 (2017) 495–503. https://doi.org/10.1016/j.applthermaleng.2016.08.181

[14] Y. Zhao, Z.M. Xu, B.B. Wang, J.J. He, Scale inhibition performance of sodium carboxymethyl cellulose on heattransfer surface at various temperatures: Experiments and moleculardynamics simulation. International Journal of Heat and Mass Transfer 141 (2019) 457–463. https://doi.org/10.1016/j.ijheatmasstransfer.2019.06.091

[15] Z.M. Xu, Y. Zhao, J.T. Wang, H.L. Chang, Inhibition of calcium carbonate fouling on heat

transfer surface usingsodium carboxymethyl cellulose. Applied Thermal Engineering 148 (2019) 1074–1080. https://doi.org/10.1016/j.applthermaleng.2018.11.088
[16] J.Quarini, Ice-pigging to reduce and remove fouling and to achieve clean-in-place. Applied Thermal Engineering 22(7) (2002) 747–753. https://doi.org/10.1016/S1359-4311(02)00019-4
[17] Flávia C. C. Moura, Regiane D. F. Rios, Breno R. L. Galvão, Emerging contaminants removal by granular activated carbon obtainedfrom residual Macauba biomass. Environmental Science and Pollution Research volume 25, pages26482–26492(2018) https://doi.org/10.1007/s11356-018-2713-8
[18] C.H.Sohn, C.S.Kim, S.Y.Moon, Y.I.Cho, Effect of a longitudinally positioned solenoid coil on electronic descaling. International Communications in Heat and Mass Transfer. 32(1-2)(2005)240-247. https://doi.org/10.1016/j.icheatmasstransfer.2004.06.009
[19] Y.I. Cho, H.S. Kim, Zahid Amjad, Kostas Demadis (Eds.), Nonchemical Methods to Control Scale and Deposit Formation, Mineral Scales and Deposits, Scientific and Technological Approaches, 2015, pp. 193–221 Chapter 9. https://doi.org/10.1016/B978-0-444-63228-9.00009-7
[20] G. JaeLee, L.D.Tijing, B. ChoonPak, B. JoonBaek. Use of catalytic materials for the mitigation of mineral fouling. International Communications in Heat and Mass Transfer. 33(1)(2006)14-23. https://doi.org/10.1016/j.icheatmasstransfer.2005.08.011.
[21] R.D. Ambashta, M.Sillanpää, Water purification using magnetic assistance: A review. Journal of Hazardous Materials 180 (2010) 38–49. https://doi.org/10.1016/j.jhazmat.2010.04.105
[22] HH Ge，XM Gong，R Liu，XJ Meng (Eds.), Scale inhibition of electromagnetic water treatment and corrosion behavior of carbon steel in simulated water. International Conference on Bioinformatics & Biomedical Engineering. 2010. DOI: 10.1109/ICBBE.2010.5514918
[23] W.Kim, D.J.Cho, Y.I.Cho, Use of RF electric fields for simultaneous mineral and bio-fouling control in a heat exchanger. International Communications in Heat and Mass Transfer. 38(8)20111003-1007. https://doi.org/10.1016/j.icheatmasstransfer.2011.05.007
[24] K.H. Teng, S.N. Kazi, A. Amir, A.F. Habal (Eds.), Calcium carbonate fouling on double-pipe heat exchanger with differentheat exchanging surfaces. Powder Technology 315 (2017) 216–226. https://doi.org/10.1016/j.powtec.2017.03.057
[25] Z.M. Xu, J.T. Wang, Y.T. Jia X.Y. Geng(Eds.), Experimental study on microbial fouling characteristics of the plate heat exchanger. Applied Thermal Engineering 108 (2016) 150–157. https://doi.org/10.1016/j.applthermaleng.2016.07.110

Pressure of design	Test of design	Heat exchange area	Temperature	Material
1.6MPa	2MPa	121m2	150℃	316L

Table 1 parameters of plate heat exchanger.

Operating parameters of heat exchange station	
Heat exchanger form	Plate heat exchanger
Primary network supply water temperature	60-90℃
Primary network return water temperature	35-45℃
Secondary network water supply temperature	33-45℃
Secondary network return water temperature	28-38℃
Primary network inlet and outlet pipe diameter	400mm
Diameter of inlet and outlet of secondary network	200mm
Average velocity of primary network	0.5m/s
Average flow rate of secondary network	2.3m/s
usage time	3 Years

Table 2 parameters of experimental system operating

Time(h)	Fouling resistance of heat exchanger B(m^2K/W)	Fouling resistance of heat exchanger A(m^2K/W)	reduction rate (%)
100	2.6×10-4	3.29×10-4	21.07
200	2.88×10-4	4.33×10-4	33.49
300	3.02×10-4	4.54×10-4	33.42
400	3.27×10-4	5.25×10-4	37.75
500	3.50×10-4	6.19×10-4	43.43
600	3.58×10-4	7.29×10-4	50.95
700	3.53×10-4	8.00×10-4	55.95
800	3.50×10-4	8.44×10-4	58.47
850	3.58×10-4	8.54×10-4	58.04

Table 3. The fouling resistance on the heat exchanger surface every 100 hours after the system is stable.

Element	Scale weight of heat exchanger A(%)	Scale weight of heat exchanger B(%)	Weight gain(%)
C	9.06	17.48	8.42
O	39.10	47.67	7.57
Si	2.94	4.09	1.15
Ca	0.71	1.70	0.99
Fe	48.18	28.40	-19.78
Cu		0.66	0.66

Table 4 EDS data analysis and variation of scale

Figures

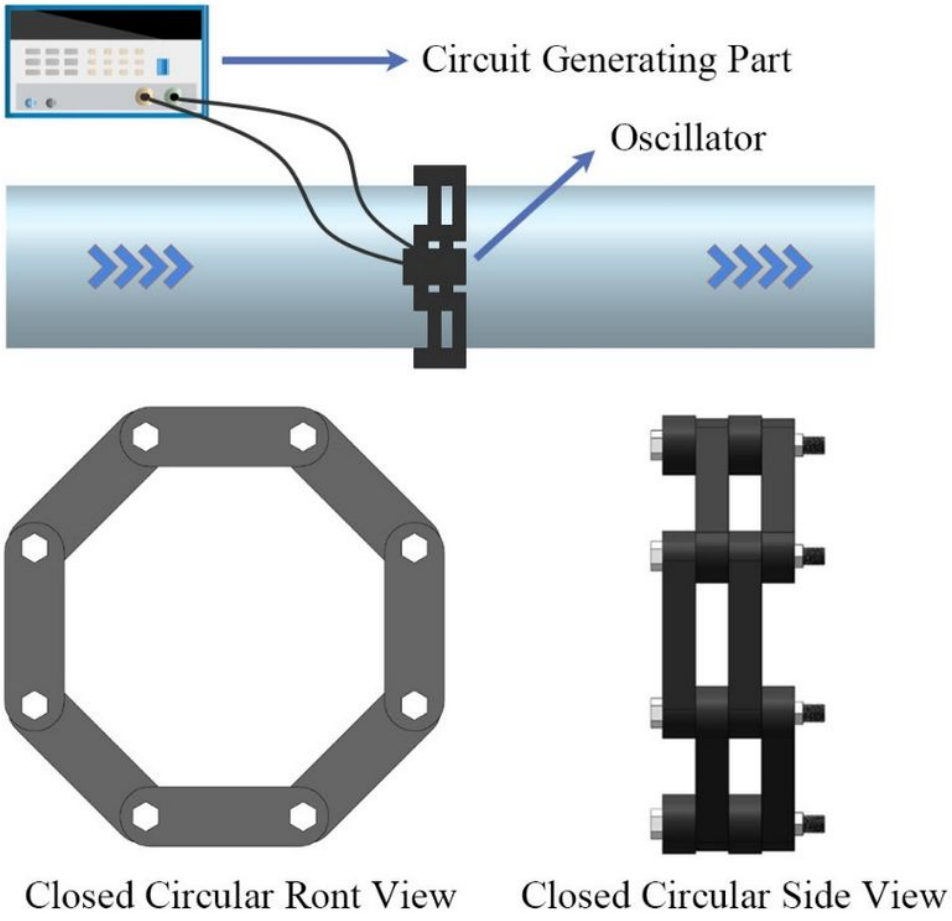

Figure 1

A diagram of the alternating variable frequency electric field device schematic

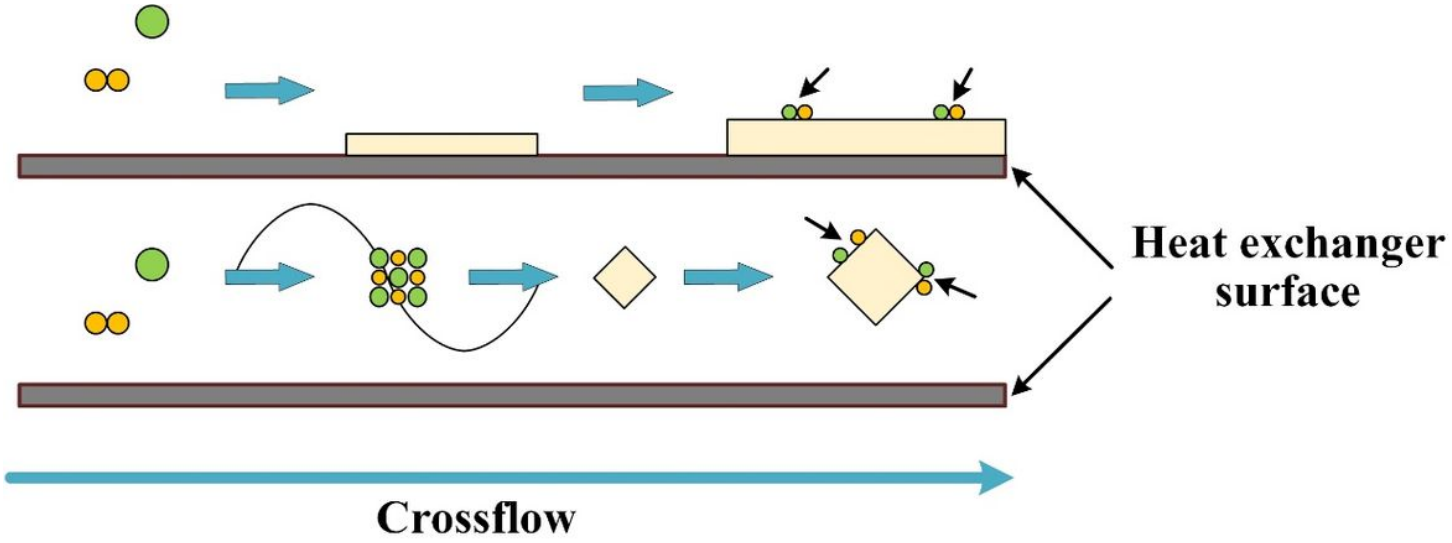

Figure 2

Schematic diagram of electric field inhibition scale process

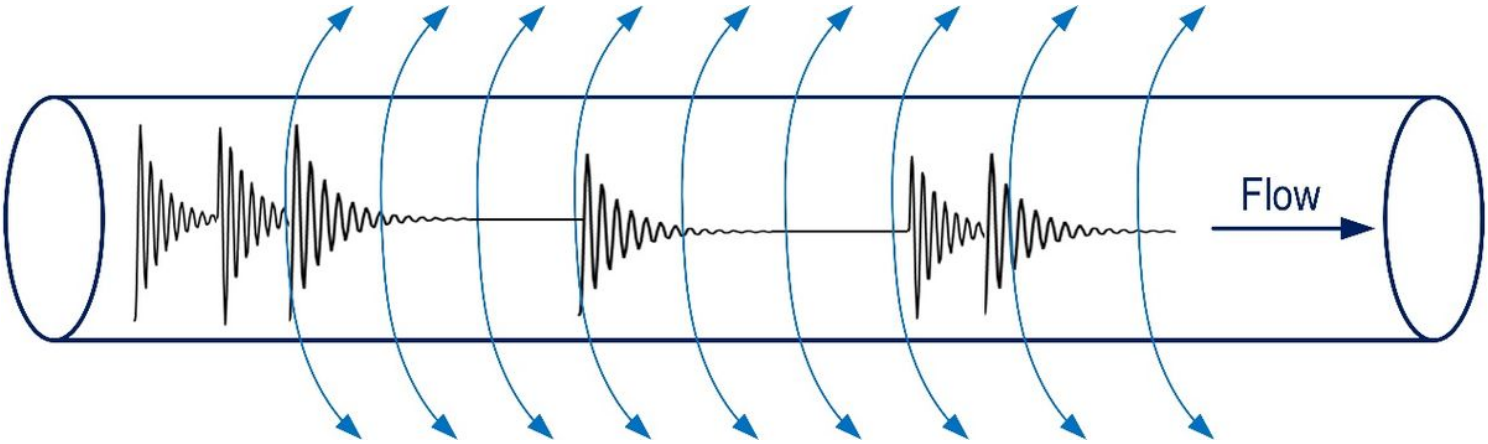

Figure 3

A diagram of the waveform of underdamped attenuated oscillation signal

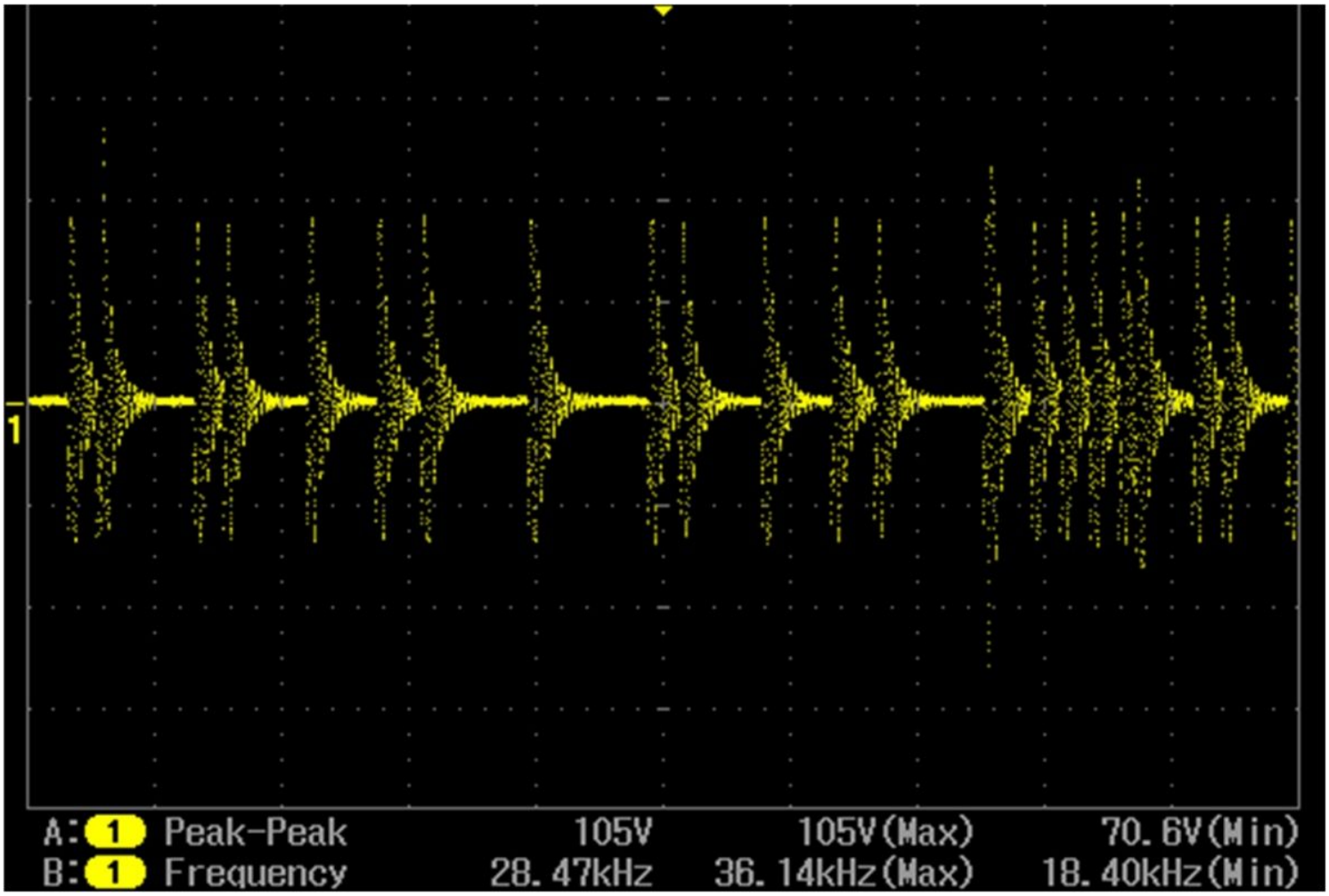

Figure 4

A diagram of the underdamped attenuated oscillating signal waveform in oscilloscope

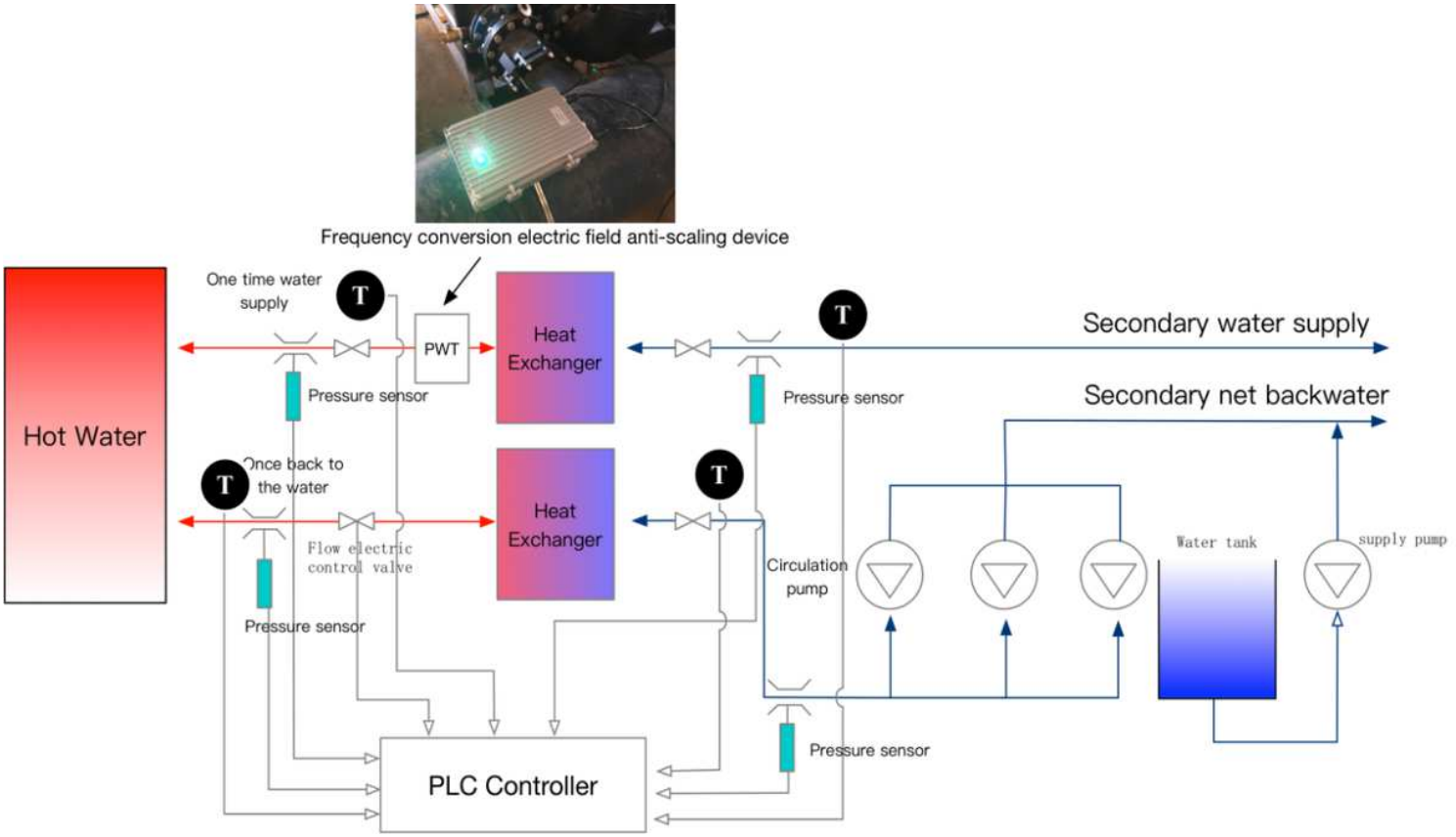

Figure 6

A diagram of the scale inhibition test flowloop

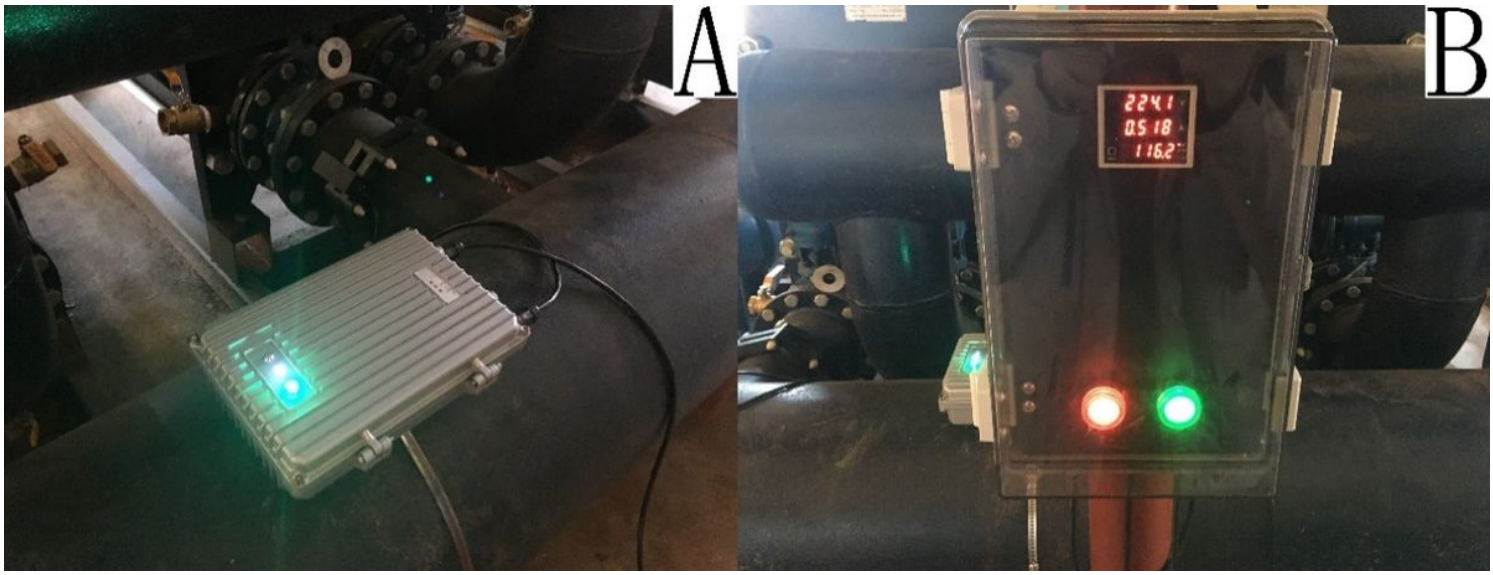

Figure 7

A diagram of the field test installation

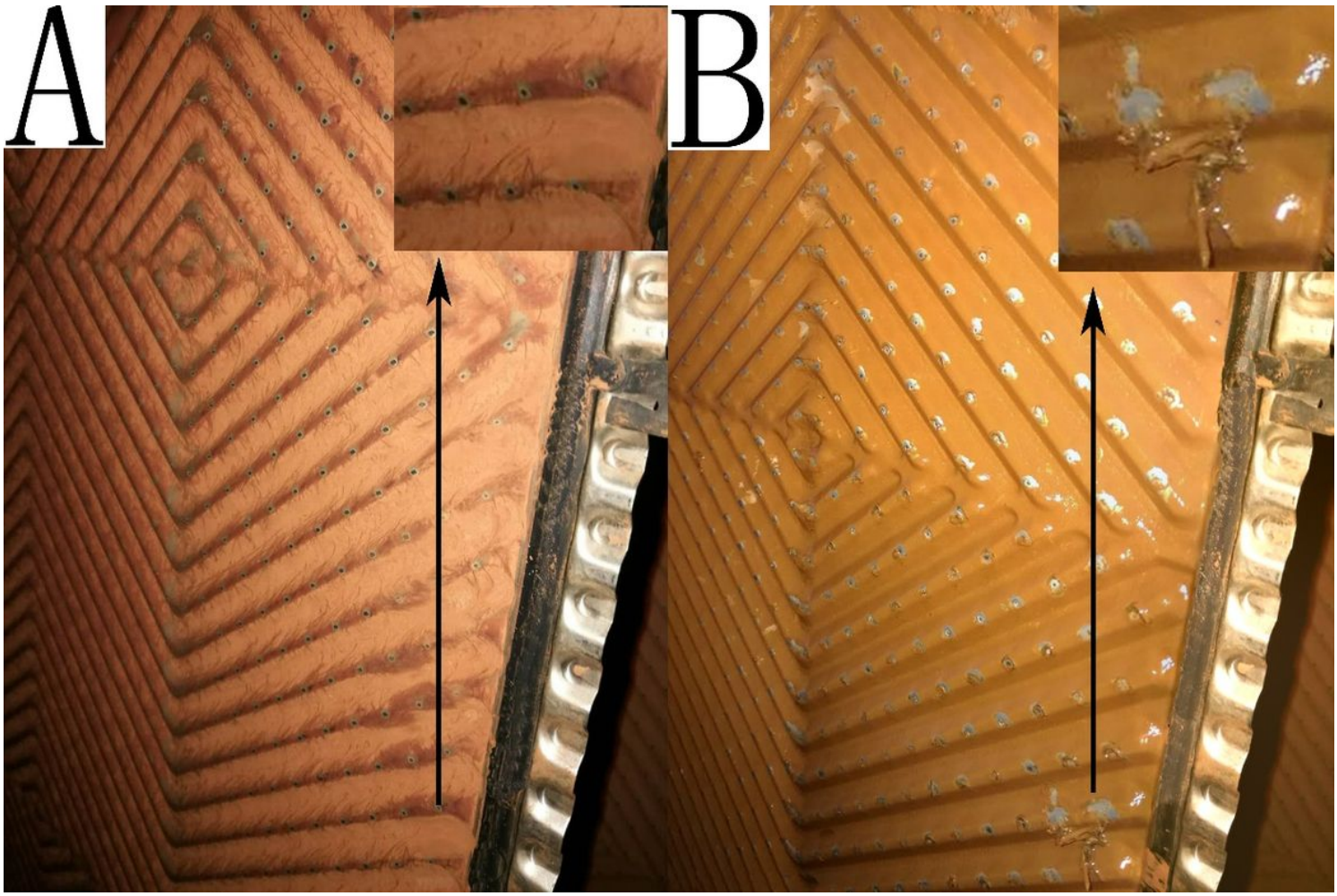

Figure 8

Comparison of scale of plate heat exchangers

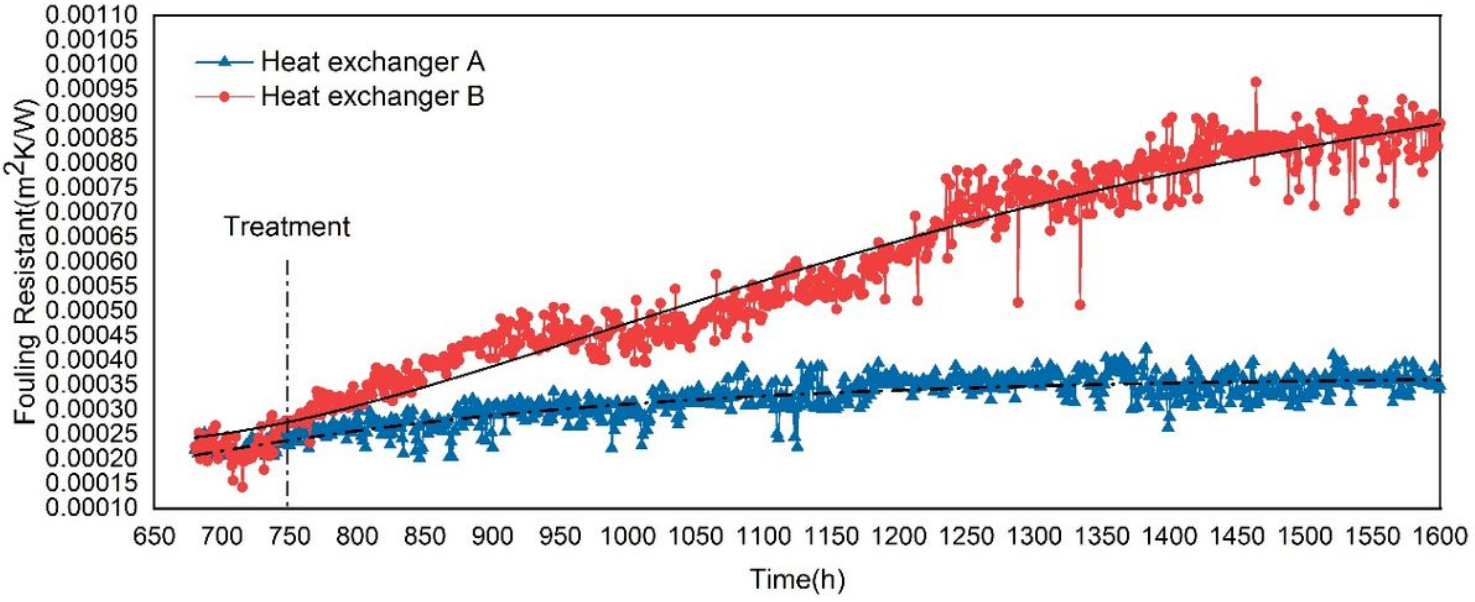

Figure 9

Changes in the fouling resistance on the heat exchanger surface in the test

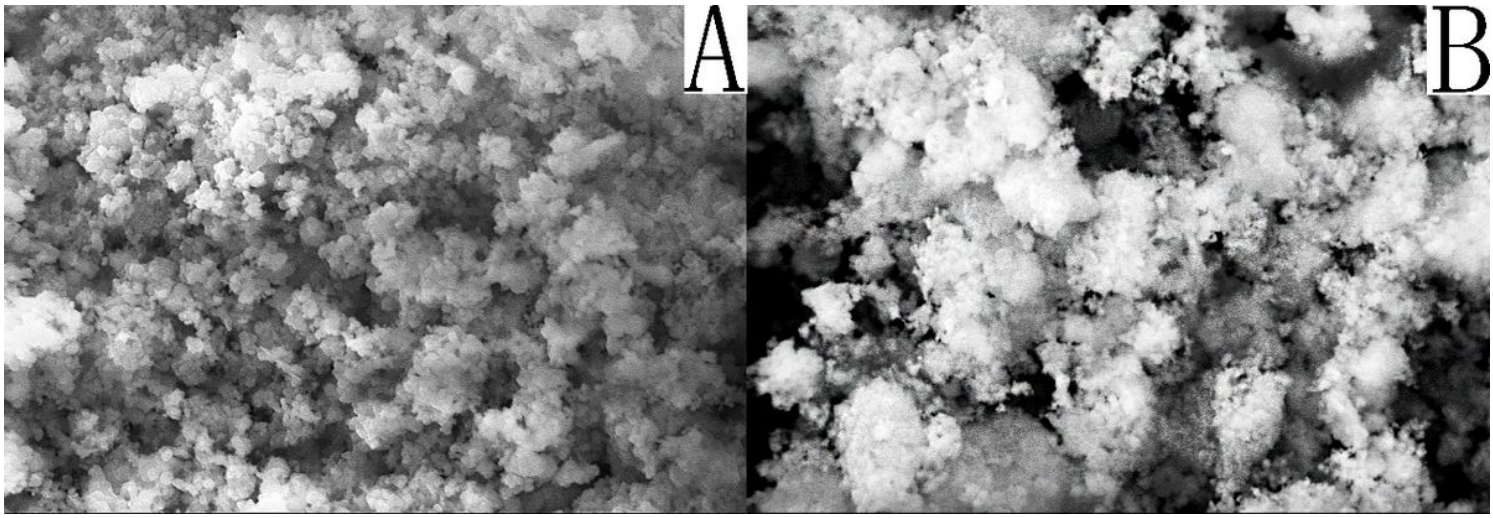

Figure 10

SEM image of scale on heat exchanger surface

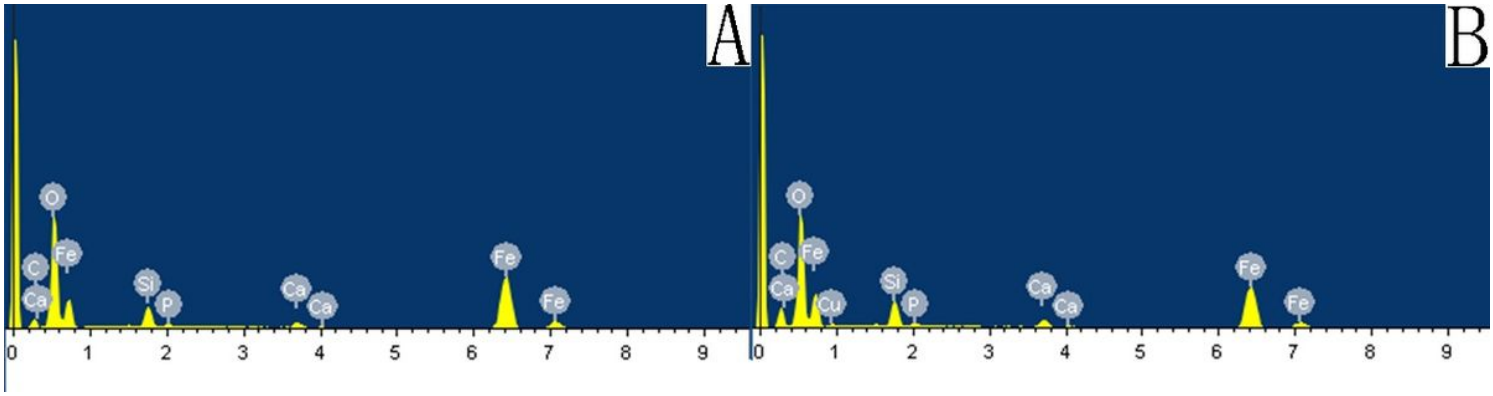

Figure 11

Comparison of EDS of scale on heat exchanger surface